IJREAT International Journal of Research in Engineering & Advanced Technology, Volume 3, Issue 1, Feb-Mar, 2015
ISSN: 2320 – 8791 (Impact Factor: 1.479)
www.ijreat.org

Robust Nonlinear Backstepping Controller Design for Doubly-Fed Induction Machine in Wind Power Generation

Mohammed Rachidi[1], Badr Bououlid Idrissi[2]

[1,2]**Département of Electromechanical Engineering,** ***Moulay Ismaïl University, Ecole Nationale Supérieure d'Arts et Métiers, BP 4024, Marjane II, Beni Hamed, 50000, Meknès, Morocco***

Abstract

In this paper, a robust nonlinear backstepping speed and current controller was proposed for Doubly-Fed Induction Generator (DFIG) in wind power generation. To achieve maximum power extraction, commonly referred to as 'Maximum Power Point Tracking' (MPPT), the rotor speed was changed in response to the changing wind speed to continuously operate the wind turbine at its optimum Tip Speed Ratio. The dynamic model was based on field orientation principle and both certain (known parameters) and uncertain (unknown mechanical parameters) cases were considered. The mathematical development of the controller design was examined in detail. The overall stability of the system was shown using Lyapunov Technique. Computer simulation results obtained and comparison with conventional backstepping confirmed the robustness, effectiveness and validity of the proposed control.

Keywords: *Wind Power Generation, MPPT, Doubly-Fed Induction Generator, Robust Adaptive Backstepping, unknown mechanical parameter, Lyapunov Technique.*

1. Introduction

The grid-connected doubly fed induction generator is an emerging technology, used in variable-speed large wind turbines. The most attractive feature of such a system is that only 20 to 30% of the power needs to pass through frequency conversion in the rotor circuit, which gives a substantial reduction in the power electronics cost as compared with the variable-speed synchronous generator. Additionally variable speed operation allows to continuously operating the wind turbine at its optimum Tip Speed Ratio (TSR), which is specific to the aerodynamic design of a given turbine. This achieves maximum rotor efficiency and hence maximum power extraction. Experience indicates that the variable-speed operation yields 20 to 30% more power than with the fixed-speed operation. Other benefits of this configuration include smooth grid connection, drive train load reduction and separate control of active and reactive power. DFIG drive system uses back-to-back converters in the rotor circuit which decouple the rotor speed and grid frequency (fig.1). Such a configuration gives wider range of variable speed of approximately ± 30% around synchronous speed [1-2].

This paper introduces an adaptive nonlinear backstepping controller based on field orientation for DFIG drive system. The idea of backstepping design is to select recursively some appropriate functions of state variables as pseudo-control inputs for lower dimension subsystems of the overall system. Each backstepping stage results into a new pseudo-control design, expressed in terms of the pseudo-control designs from the preceding design stages. When the procedure terminates, a feedback design for the true control input results and achieves the original design objective by virtue of a Lyapunov function, which is formed by summing up the Lyapunov functions associated with each individual design stage [3-5]. The proposed controller ensures speed and current tracking objective under unknown mechanical parameters. The reminder of the paper is divided into four sections. The second section presents the DFIG drive system. The third section describes the mathematical model of wind generation system. In the fourth section the mathematical development of the controller design is examined with sufficient depth. In the last section, some simulation results are presented which confirm the effectiveness and the validity of the proposed control.

2. Variable-speed DFIG drive system

The wind turbine and the doubly-fed induction generator are shown in the figure 1. The AC/DC/AC converter is divided into two components: the rotor-side converter (C_{rotor}) and the grid-side converter (C_{grid}). C_{rotor} and C_{grid} are Voltage-Sourced Converters that use forced-commutated power electronic devices (IGBTs) to

synthesize an AC voltage from a DC voltage source. A capacitor connected on the DC side acts as the DC voltage source. A coupling inductor R-L is used to connect C_{grid} to the grid. The three-phase rotor winding is connected to C_{rotor} by slip rings and brushes and the three-phase stator winding is directly connected to the grid. The power captured by the wind turbine is converted into electrical power by the induction generator and it is transmitted to the grid by the stator and the rotor windings. The control system generates the pitch angle command and the voltage command signals V_r and V_{gc} for C_{rotor} and C_{grid} respectively in order to control the power of the wind turbine, the DC bus voltage and the reactive power at the grid terminals.

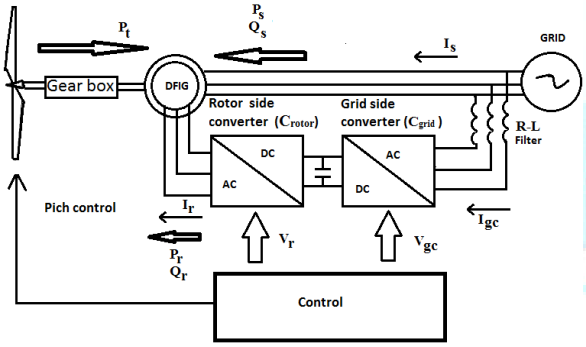

Fig.1: Wind energy conversion system

In this figure the followings parameters are used:

P_t: Mechanical power captured by the wind turbine and transmitted to the rotor

P_s: Stator electrical power output

P_r: Rotor electrical power output

P_{gc}: C_{grid} electrical power output

Q_s: Stator reactive power output

Q_r: Rotor reactive power output

Q_{gc}: C_{grid} reactive power output

T_t: Mechanical torque applied to rotor

T_{em}: Electromagnetic torque applied to the rotor by the generator

Ω: Rotational speed of rotor

Ωs: Rotational speed of the magnetic flux in the air-gap of the generator, this speed is named synchronous speed. It is proportional to the frequency of the grid voltage and to the number of generator poles.

The mechanical power is given by:

$$P_t = T_t\ \Omega \qquad (1)$$

The power output is computed as follows:

$$P_s = T_{em}\ \Omega_s \qquad (2)$$

In steady-state at fixed speed for a loss less generator:

$$T_t = -T_{em} \qquad (3)$$

$$P_t = -(P_s + P_r) \qquad (4)$$

It follows that:

$$P_r = -P_t - P_s = -gP_s \qquad (5)$$

Where g is defined as the slip of the Generator:

$$g = \frac{\Omega_s - \Omega}{\Omega_s}$$

Generally the absolute value of slip is much lower than 1 and, consequently, P_r is only a fraction of P_s. Since T_t is positive for power generation and since Ω_s is positive and constant for a constant frequency grid voltage, P_s is negative, the sign of P_r is a function of the slip sign. P_r is negative for negative slip (speed greater than synchronous speed) and it is positive for positive slip (speed lower than synchronous speed). For super-synchronous speed operation, P_r is transmitted to DC bus capacitor and tends to rise the DC voltage. For sub-synchronous speed operation, P_r is taken out of DC bus capacitor and tends to decrease the DC voltage. C_{grid} is used to generate or absorb the power P_{gc} in order to keep the DC voltage constant. In steady-state for a loss less AC/DC/AC converter P_{gc} is equal to P_r and the speed of the wind turbine is determined by the power P_r absorbed or generated by C_{rotor}.

3. Modeling of the wind generation system

3.1. Modeling of the wind turbine

The aerodynamic turbine power P_t depends on the power coefficient C_p as follows [6]:

$$P_t = \frac{1}{2}\rho\,\pi\,R^2\,C_p(\lambda,\beta)\,v^3 \qquad (6)$$

where:
ρ: Specific mass of the air (kg/m^2);
v: Wind speed (m/s);
R: Radius of turbine (m);
Cp: Power coefficient;
β: Blade pitch angle (deg);
Ω: Generator speed (rad/s);
λ: Tip Speed Ratio (TSR) of the rotor blade tip speed to wind speed.

The TSR is given by:

$$\lambda = \frac{R\,\Omega}{G\,v} \qquad (7)$$

where G is Mechanical speed multiplier. A generic equation is used to model $c_p(\lambda,\beta)$, based on the modeling turbine characteristics of [6]:

$$C_p(\lambda,\beta) = c_1\left(\frac{c_2}{\lambda_i} - c_3\beta - c_4\right)e^{-\frac{c_5}{\lambda_i}} + c_6\lambda \qquad (8)$$

where $\frac{1}{\lambda_i} = \frac{1}{\lambda + 0.08\beta} - \frac{0.035}{\beta^3 + 1}$ and the coefficients c_1 to c_6 are: c_1 = 0.5176, c_2 = 116, c_3 = 0.4, c_4 = 5, c_5 = 21 and c_6 = 0.0068.

The C_p-λ characteristics, for different values of the pitch angle β, are illustrated in figure 2. Then the maximum value of c_p (c_{pmax}= 0.48) is achieved for β = 0 degree and for λ = λ_{opt} =8.1.

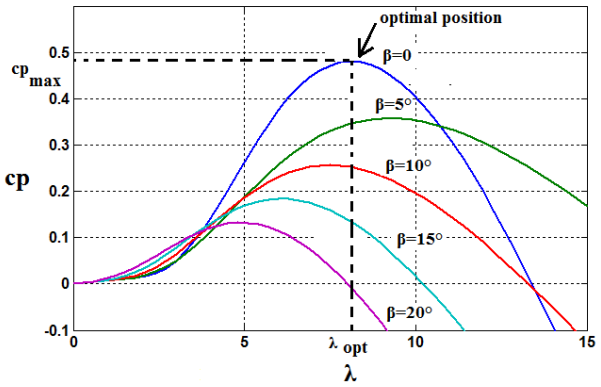

Fig.2: Power coefficient Cp(β, λ)

3.2. MPPT Strategy

In this work, we assume that the wind turbine operates with β=0. To capture the maximum power, a speed controller must control the mechanical speed Ω in order to get a speed reference Ω_c that keeps the system at λ_{opt}.

According to (6) and (7), it is possible to deduce in real time the speed reference and the optimal mechanical power which can be generated using the maximum power point tracking (MPPT) as:

$$\begin{cases} \Omega_c = \dfrac{G\,v}{R\,\lambda_{opt}} \\ P_{\max} = \dfrac{1}{2}\rho\,\pi\,R^2 C_{p\max}\,v^3 \end{cases} \qquad (9)$$

3.3. Modeling of Doubly-Fed Induction Generator

The induction machine is controlled in a synchronously rotating dq axis frame, with the d-axis oriented along the stator-flux vector position (ϕ_{sq}=0). The classical electrical equations are written as follows [10,11]:

$$\begin{cases} v_{sd} = R_s i_{sd} + \dfrac{d\phi_{sd}}{dt} \\ v_{sq} = R_s i_{sq} + \omega_s \phi_{sd} \\ v_{rd} = R_r i_{rd} + \dfrac{d\phi_{rd}}{dt} - \omega_r \phi_{rq} \\ v_{rq} = R_r i_{rq} + \dfrac{d\phi_{rq}}{dt} + \omega_r \phi_{rd} \end{cases} \qquad (10)$$

ω_r denotes the rotor electrical speed and is given by:

$$\omega_r = \omega_s - p\Omega \qquad (11)$$

where p is the pole pairs and ω_s is the grid pulsation.

The stator and rotor flux can be expressed as:

$$\begin{cases} \phi_{sd} = L_s i_{sd} + L_m i_{rd} \\ 0 = L_s i_{sq} + L_m i_{rq} \\ \phi_{rd} = L_r i_{rd} + L_m i_{sd} \\ \phi_{rq} = L_r i_{rq} + L_m i_{sq} \end{cases} \qquad (12)$$

The electromagnetic torque is expressed as:

$$T_{em} = -\frac{3}{2}p\frac{L_m}{L_s} i_{rq}\phi_{sd} \qquad (13)$$

The stator and rotor active and reactive powers are given by:

$$\begin{cases} P_s = \frac{3}{2}(v_{sd} i_{sd} + v_{sq} i_{sq}) \\ Q_s = \frac{3}{2}(v_{sq} i_{sd} - v_{sd} i_{sq}) \\ P_r = \frac{3}{2}(v_{rd} i_{rd} + v_{rq} i_{rq}) \\ Q_r = \frac{3}{2}(v_{rq} i_{rd} - v_{rd} i_{rq}) \end{cases} \quad (14)$$

The motion equation is given by:

$$J \frac{d\Omega}{dt} = T_t + T_{em} - f\Omega \quad (15)$$

Where J is the system inertia, T_{em} is the generator torque, T_t is the turbine torque and f is the system damping coefficient.

Since the stator is connected to the grid, and the influence of the stator resistance is small, the stator-fluxcan be considered constant and is at quadrature of the stator voltage [7-8].

$$v_{sd} = 0; \quad v_{sq} = V; \quad \phi_{sd} = \phi = \frac{V}{\omega_s} \quad (16)$$

The simplified model of the wind generation system can be written as:

$$\begin{cases} \frac{di_{rd}}{dt} = av_{rd} - bi_{rd} + \omega_r i_{rq} = f_1 + av_{rd} \\ \frac{di_{rq}}{dt} = av_{rq} - bi_{rq} - \omega_r i_{rd} - c\omega_r\phi = f_2 + av_{rq} \\ \frac{d\Omega}{dt} = \frac{T_t}{J} - F\Omega + \frac{ki_{rq}}{J} \end{cases} \quad (17)$$

where:

$$f_1 = -bi_{rd} + \omega_r i_{rq}\ ; f_2 = -bi_{rq} - \omega_r i_{rd} - c\omega_r\phi$$

and

$$F = \frac{f}{J}\ ;\ k = -\frac{3}{2} p \frac{L_m}{L_s}\phi\ ;\quad \sigma = 1 - \frac{L_m^2}{L_s L_r}\ ;\quad a = \frac{1}{\sigma L_r}\ ;\ b = aR_r\ ;$$

$$c = a\frac{L_m}{L_s}\ .$$

Using (14) and (16) the stator and rotor active and reactive powers become:

$$\begin{cases} P_s = -\frac{3L_m}{2L_s} V i_{rq} \\ Q_s = \frac{3V^2}{2L_s\omega_s} - \frac{3L_m}{2L_s} V i_{rd} \end{cases} \quad (18)$$

Stator reactive power can be controlled by i_{rd} and the stator active power will be controlled by i_{rq}.

4. Control design

According to (17), the proposed schematic control is:

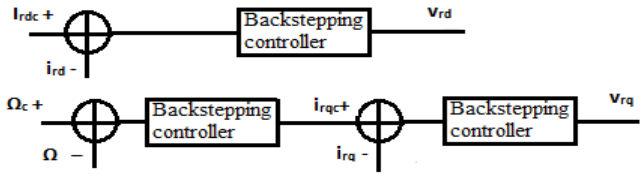

Fig.3: Block diagram of the proposed controller

4.1. Conventional backstepping (certain model)

In this case system parameters are assumed to be known including mechanical parameters. The calculation of the control variables v_{rd} and v_{rq} is done in accordance with the Figure 3 [4,5].

a- Control variable v_{rd}

The error variable is:

$$e_1 = i_{rdc} - i_{rd} \quad (19)$$

According to (17), the dynamic equation of the error is:

$$\dot{e}_1 = \dot{i}_{rdc} - f_1 - av_{rd} \quad (20)$$

To reduce the tracking error, we use the following Lyapunov candidate function:

$$V_1 = \frac{1}{2}e_1^2 \quad (21)$$

The derivative of V_1 is given by:

$$\dot{V}_1 = e_1 \dot{e}_1 \quad (22)$$

The choice $\dot{e}_1 = -k_1 e_1$ with $k_1 > 0$ verify the condition of attractiveness since $\dot{V}_1$ becomes: $\dot{V}_1 = -k_1 e_1^2 \le 0$.
Using (20), the control variable v_{rd} is given by:

$$v_{rd} = \frac{\dot{i}_{rdc} - f_1 + k_1 e_1}{a} \quad (23)$$

b- Control variable v_{rq}

The calculation is done in two steps:

Step1: Virtual control variable i_{rqc}.

The error variable e_2 is defined by:

$$e_2 = \Omega_c - \Omega \tag{24}$$

According to (17), the dynamic equation of the error is:

$$\dot{e}_2 = \dot{\Omega}_c - \frac{T_t}{J} + F\Omega - \frac{ki_{rq}}{J} \tag{25}$$

To reduce the tracking error, we use the following Lyapunov candidate function:

$$V_2 = \frac{1}{2}e_2^2 \tag{26}$$

The derivative of V_2 is given by:

$$\dot{V}_2 = e_2\dot{e}_2 \tag{27}$$

The choice $\dot{e}_2 = -k_2 e_2$ with $k_2>0$ verify the condition of attractiveness since $\dot{V}_2$ becomes: $\dot{V}_2 = -k_2 e_2^2 \le 0$.
Using (25) and (17), the virtual control variable i_{rqc} is given by:

$$i_{rqc} = \frac{J(\dot{\Omega}_c + F\Omega + k_2 e_2)}{k} - \frac{T_t}{k} \tag{28}$$

Step2: Control variable v_{rq}

The error variable e_3 is defined by:

$$e_3 = i_{rq_c} - i_{rq} \tag{29}$$

Equation (25) can be rewritten as:

$$\dot{e}_2 = \dot{\Omega}_c - \frac{T_t}{J} + F\Omega - \frac{ki_{rqc}}{J} + \frac{k}{J}(i_{rqc} - i_{rq}) \tag{30}$$

Using (28) and (29):

$$\dot{e}_2 = -k_2 e_2 + \frac{k}{J}e_3 \tag{31}$$

Taking the derivative of (29) and using (28), (17) gives:

$$\begin{aligned}\dot{e}_3 &= \frac{J(\ddot{\Omega}_c + F\dot{\Omega} + k_2\dot{e}_2)}{k} - \frac{\dot{T}_t}{k} - f_2 - av_{rq} \\ &= A - av_{rq}\end{aligned} \tag{32}$$

where the A term is given by (using Equ. (17)):

$$A = \frac{J(\ddot{\Omega}_c + F(\frac{T_t}{J} - F\Omega + \frac{ki_{rq}}{J}) + k_2(-k_2 e_2 + \frac{k}{J}e_3)}{k} - \frac{\dot{T}_t}{k} - f_2 \tag{33}$$

To reduce the tracking error, we use the following Lyapunov candidate function:

$$V = \frac{1}{2}e_1^2 + \frac{1}{2}e_2^2 + \frac{1}{2}e_3^2 \tag{34}$$

The derivative of V is given by:

$$\begin{aligned}\dot{V} &= e_1\dot{e}_1 + e_2\dot{e}_2 + e_3\dot{e}_3 \\ &= e_1(-k_1 e_1) + e_2(-k_2 e_2 + \frac{k}{J}e_3) + e_3(A - av_{rq}) \\ &\quad + k_3 e_3^2 - k_3 e_3^2 \\ &= -k_1 e_1^{\,2} - k_2 e_2^2 - k_3 e_3^2 + e_3(k_3 e_3 \\ &\quad + \frac{k}{J}e_2 + A - av_{rq})\end{aligned} \tag{35}$$

The choice,

$$v_{rq} = \frac{k_3 e_3 + \frac{k}{J}e_2 + A}{a} \tag{36}$$

with $k_3>0$ verify the condition of attractiveness since $\dot{V}$ becomes $\dot{V} = -k_1 e_1^{\,2} - k_2 e_2^2 - k_3 e_3^2 \le 0$.

4.2. Robust Adaptive Backstepping (uncertain model)

In the case of uncertain model where system parameters are not known with enough accuracy or vary with time, suitable choice of control variables and update laws must be done to still ensure the attractiveness condition [8,9]. The study focuses on the variations of the mechanical parameters F and J. The estimated parameters are denoted respectively by $\hat{F}(t)$ and $\hat{J}(t)$. Errors of estimate are defined by:

$$\begin{aligned}\tilde{J} &= \hat{J} - J \\ \tilde{F} &= \hat{F} - F\end{aligned} \tag{37}$$

Lemma: *The following control variables and update laws,*

$$\begin{aligned}&v_{rd} = \frac{\dot{i}_{rdc} - f_1 + k_1 e_1}{a},\ v_{rq} = \frac{\psi_2 + k_3 e_3}{a} \\ &\dot{\hat{F}} = \gamma_2(e_2\Omega + e_3\psi_4),\ \dot{\hat{J}} = -\gamma_1(e_3\psi_3 - e_2\psi_1)\end{aligned} \tag{38}$$

with

$$e_1 = i_{rdc} - i_{rd}, \quad e_2 = \Omega_c - \Omega,$$
$$e_3 = \hat{i}_{rqc} - i_{rq}, \quad \hat{i}_{rqc} = \frac{\hat{J}}{k}\psi_1 - \frac{T_t}{k},$$
$$\psi_1 = \dot{\Omega}_c + \hat{F}\Omega + k_2 e_2 ,$$
$$\psi_2 = \frac{\dot{\hat{J}}}{k}\psi_1 + \frac{\hat{J}}{k}(\ddot{\Omega}_c + \dot{\hat{F}}\Omega - \hat{F}^2\Omega - k_2^2 e_2)$$
$$+ k_2 e_3 + \hat{F}(i_{rq} + \frac{T_t}{k}) - f_2 - \frac{\dot{T}_t}{k},$$
$$\psi_3 = k_2 e_3 + \hat{F}(i_{rq} + \frac{T_t}{k}) - k_2\frac{\hat{J}}{k}\psi_1 ,$$
$$\psi_4 = \frac{\hat{J}}{k}(k_2 - \hat{F})\,\Omega ,$$

ensure the attractiveness condition despite the changes in the mechanical parameters F and J.

Proof:

a- Control variable v_{rd}

The calculation made in Section 4.1 remains valid and the control variable v_{rd} is given by Equ. 23.

b- Control variable v_{rq}

Step1: Virtual control variable $\hat{i}_{rqc}$

The error variable e_2 is defined by:

$$e_2 = \Omega_c - \Omega \qquad (39)$$

According to (17), the dynamic equation of the error is:

$$\dot{e}_2 = \dot{\Omega}_c - \frac{T_t}{J} + F\Omega - \frac{k i_{rq}}{J} \qquad (40)$$

Using (28), the virtual control variable i_{rqc} is given by:

$$i_{rqc} = \frac{J(\dot{\Omega}_c + F\Omega + k_2 e_2)}{k} - \frac{T_t}{k} \qquad (41)$$

Thus:

$$\hat{i}_{rqc} = \frac{\hat{J}(\dot{\Omega}_c + \hat{F}\Omega + k_2 e_2)}{k} - \frac{T_t}{k} = \frac{\hat{J}}{k}\psi_1 - \frac{T_t}{k} \qquad (42)$$

Where ψ_1 is given by:

$$\psi_1 = \dot{\Omega}_c + \hat{F}\Omega + k_2 e_2 \qquad (43)$$

Step2: Control variable v_{rq} and update laws $\hat{F}(t)$ and $\hat{J}(t)$

The error variable e_3 is defined by:

$$e_3 = \hat{i}_{rqc} - i_{rq} \qquad (44)$$

To select the Lyapunov candidate function, unknown parameters J and F should be eliminated from the expressions of $\dot{e}_2$ and $\dot{e}_3$.

Equation (40) can be rewritten as:

$$\dot{e}_2 = \dot{\Omega}_c - \frac{T_t}{J} + \hat{F}\Omega - \tilde{F}\Omega - \frac{k\hat{i}_{rqc}}{J} + \frac{k}{J}(\hat{i}_{rq_c} - i_{rq}) \qquad (45)$$

Using (42) and (44), (45) becomes:

$$\dot{e}_2 = \dot{\Omega}_c + \hat{F}\Omega - \tilde{F}\Omega - \frac{\hat{J}}{J}\psi_1 + \frac{k}{J}e_3 \qquad (46)$$

Since

$$\frac{\hat{J}}{J}\psi_1 = \frac{\tilde{J}}{J}\psi_1 + \psi_1 \qquad (47)$$

Using (43), (46) becomes:

$$\dot{e}_2 = -k_2 e_2 - \tilde{F}\Omega - \frac{\tilde{J}}{J}\psi_1 + \frac{k}{J}e_3 = B - \frac{\tilde{J}}{J}\psi_1 + \frac{k}{J}e_3 \qquad (48)$$

where $B = -k_2 e_2 - \tilde{F}\Omega$.

Likewise:

$$e_3 = \frac{\hat{J}}{k}\psi_1 - \frac{T_t}{k} - i_{rq} \qquad (49)$$

Taking the derivative of e_3 and using (17) give:

$$\dot{e}_3 = \frac{\dot{\hat{J}}}{k}\psi_1 + \frac{\hat{J}}{k}\dot{\psi}_1 - \frac{\dot{T}_t}{k} - f_2 - a v_{rq} \qquad (50)$$

On the other hand, the derivative of ψ_1 gives (Equ. 43):

$$\dot{\psi}_1 = \ddot{\Omega}_c + \dot{\hat{F}}\Omega + \hat{F}\dot{\Omega} + k_2\dot{e}_2 \qquad (51)$$

According to (17) :

$$\dot{\Omega} = \frac{T_t}{k} - F\Omega + \frac{k i_{rq}}{J} = -\hat{F}\Omega + \tilde{F}\Omega + \frac{k i_{rq} + T_t}{J} = C + \frac{k i_{rq} + T_t}{J} \qquad (52)$$

where $C = -\hat{F}\Omega + \tilde{F}\Omega$.

Thus, using (48) and (52):

$$\dot{\psi}_1 = \ddot{\Omega}_c + \dot{\hat{F}}\Omega + \hat{F}(C + \frac{ki_{rq} + T_l}{J}) + k_2(B - \frac{\tilde{J}}{J}\psi_1 + \frac{k}{J}e_3)$$
$$= \ddot{\Omega}_c + \dot{\hat{F}}\Omega + \hat{F}C + k_2B + \frac{k}{J}(\hat{F}(i_{rq} + \frac{T_l}{k}) + k_2e_3) - k_2\frac{\tilde{J}}{J}\psi_1 \text{ where}$$
$$= D + \frac{k}{J}(\hat{F}(i_{rq} + \frac{T_l}{k}) + k_2e_3) - k_2\frac{\tilde{J}}{J}\psi_1 \quad (53)$$
$$D = \ddot{\Omega}_c + \dot{\hat{F}}\Omega + \hat{F}C + k_2B .$$

Equation (50) becomes:

$$\dot{e}_3 = \frac{\dot{\hat{J}}}{k}\psi_1 + \frac{\hat{J}}{k}D + \frac{\hat{J}}{J}(\hat{F}(i_{rq} + \frac{T_l}{k}) + k_2e_3) - \frac{\tilde{J}}{J}(k_2\frac{\hat{J}}{k}\psi_1) - f_2$$
$$- av_{rq} - \frac{\dot{T}_l}{k}$$
$$= \frac{\dot{\hat{J}}}{k}\psi_1 + \frac{\hat{J}}{k}D + (1 + \frac{\tilde{J}}{J})(\hat{F}(i_{rq} + \frac{T_l}{k}) + k_2e_3) - \frac{\tilde{J}}{J}(k_2\frac{\hat{J}}{k}\psi_1)$$
$$- f_2 - av_{rq} - \frac{\dot{T}_l}{k}$$
$$= \frac{\dot{\hat{J}}}{k}\psi_1 + \frac{\hat{J}}{k}D + \hat{F}(i_{rq} + \frac{T_l}{k}) + k_2e_3 + \frac{\tilde{J}}{J}(\hat{F}(i_{rq} + \frac{T_l}{k}) + k_2e_3$$
$$- k_2\frac{\hat{J}}{k}\psi_1) - f_2 - av_{rq} - \frac{\dot{T}_l}{k} \quad (54)$$

The D term can be expressed by:

$$D = \ddot{\Omega}_c + \dot{\hat{F}}\Omega + \hat{F}C + k_2B$$
$$= \ddot{\Omega}_c + \dot{\hat{F}}\Omega + \hat{F}(-\hat{F}\Omega + \tilde{F}\Omega) + k_2(-k_2e_2 - \tilde{F}\Omega) \quad (55)$$
$$= \ddot{\Omega}_c + \dot{\hat{F}}\Omega - \hat{F}^2\Omega - k_2^2e_2 - \tilde{F}(k_2 - \hat{F})\Omega$$

Using(55), equation (54) can be written as:

$$\dot{e}_3 = \psi_2 - av_{rq} + \frac{\tilde{J}}{J}\psi_3 - \tilde{F}\psi_4 \quad (56)$$

where:

$$\begin{cases} \psi_2 = \frac{\dot{\hat{J}}}{k}\psi_1 + \frac{\hat{J}}{k}(\ddot{\Omega}_c + \dot{\hat{F}}\Omega - \hat{F}^2\Omega - k_2^2e_2) + \hat{F}(i_{rq} + \frac{T_l}{k}) \\ \qquad + k_2e_3 - f_2 - \frac{\dot{T}_l}{k} \\ \psi_3 = k_2e_3 + \hat{F}(i_{rq} + \frac{T_l}{k}) - k_2\frac{\hat{J}}{k}\psi_1 \\ \psi_4 = \frac{\hat{J}}{k}(k_2 - \hat{F})\Omega \end{cases} \quad (57)$$

To reduce the tracking errors, we propose to use the following Lyapunov candidate function:

$$V = \frac{1}{2}e_1^2 + \frac{1}{2}e_2^2 + \frac{1}{2}e_3^2 + \frac{1}{2\gamma_1}\frac{\tilde{J}^2}{J} + \frac{1}{2\gamma_2}\tilde{F}^2 \quad (58)$$

Taking the derivative of V gives:

$$\dot{V} = e_1\dot{e}_1 + e_2\dot{e}_2 + e_3\dot{e}_3 + \frac{1}{\gamma_1}\frac{\tilde{J}\dot{\tilde{J}}}{J} + \frac{1}{\gamma_2}\tilde{F}\dot{\tilde{F}} - k_3e_3^2 + k_3e_3^2$$
$$= -k_1e_1^2 + e_2(-k_2e_2 - \tilde{F}\Omega - \frac{\tilde{J}}{J}\psi_1 + \frac{k}{J}e_3)$$
$$+ e_3(\psi_2 - av_{rq} + \frac{\tilde{J}}{J}\psi_3 - \tilde{F}\psi_4) + \frac{1}{\gamma_1}\frac{\tilde{J}\dot{\tilde{J}}}{J} + \frac{1}{\gamma_2}\tilde{F}\dot{\tilde{F}}$$
$$- k_3e_3^2 + k_3e_3^2 \quad (59)$$
$$= -k_1e_1^2 - k_2e_2^2 - k_3e_3^2 + \frac{k}{J}e_3e_2 + e_3(\psi_2 - av_{rq} + k_3e_3)$$
$$+ \tilde{F}(-e_2\Omega - e_3\psi_4 + \frac{\dot{\tilde{F}}}{\gamma_2}) + \frac{\tilde{J}}{J}(e_3\psi_3 - e_2\psi_1 + \frac{\dot{\tilde{J}}}{\gamma_1})$$

The choice

$$v_{rq} = \frac{\psi_2 + k_3e_3}{a}$$
$$\dot{\hat{F}} = \gamma_2(e_2\Omega + e_3\psi_4) \quad (60)$$
$$\dot{\hat{J}} = -\gamma_1(e_3\psi_3 - e_2\psi_1)$$

leads to: $\dot{V} = -k_1e_1^2 - k_2e_2^2 - k_3e_3^2 + \frac{k}{J}e_3e_2$.

To verify the condition of attractiveness, we choose:

$$\frac{k}{J} < 2\sqrt{k_2k_3} \quad (61)$$

since $\dot{V} \le -k_1e_1^2 - (\sqrt{k_2}|e_2| - \sqrt{k_3}|e_3|)^2 \le 0$.

5-Simulation results

To demonstrate the effectiveness of the proposed control schemes two SIMULINK models were constructed, which correspond respectively to the conventional (certain case) and adaptive (uncertain case) backstepping controller. The tracking capability was verified in the case of adaptive controller and sinusoidal variation of the wind speed (see Figure 4). To show the robustness against mechanical parameters change speed regulation performances by both controllers were compared at constant wind speed (see Figure 5). In all simulations constant value for the stator direct current reference was considered. Table 1 shows the design parameters used in the simulation.

Table1: Design parameters

Parameter	Value
k_1	100
k_2	100
k_3	200
γ_1	0.00006
γ_2	0.0005

Figures 4a and 4b show the good tracking capability of the adaptive controller. The slip curve (Fig. 4d) shows that both

negative and positive rotor slip are obtained which correspond respectively to negative and positive rotor power (Fig. 4c).
In figure 4e, optimal power P_{max} (Equ. 9) is compared to actual grid power Pg computed by simulation (Pg = -(Ps+Pr)). The two curves practically coincide which confirms the effectiveness of the MPPT strategy.

Figure 5 shows speed regulation performance by both conventional and adaptive controllers in the case of change in the coefficient F. The simulation assumes that changes around nominal value occur at 1s (ΔF=250%) and 2s (ΔF=200%). Unlike the conventional backstepping controller, the adaptive controller tracks the constant speed reference despite the parameter changes (Fig. 5a). This confirms the robustness of the proposed controller.

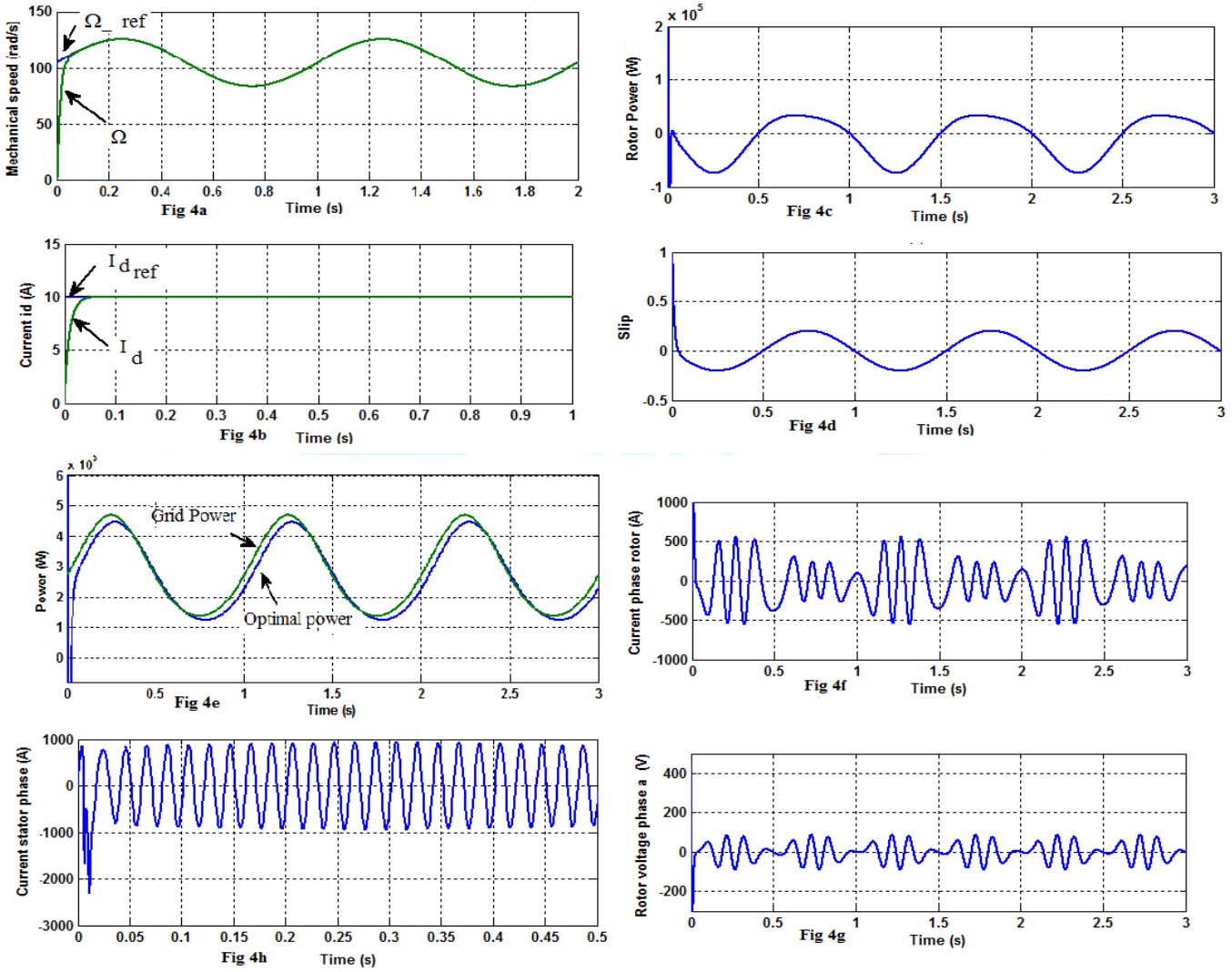

Fig.4: Tracking capability of adaptive backstepping controller
($I_{d\text{-}Ref}$=10A,$v_{wind(m/s)}$= 9.9+2sin(2πt))

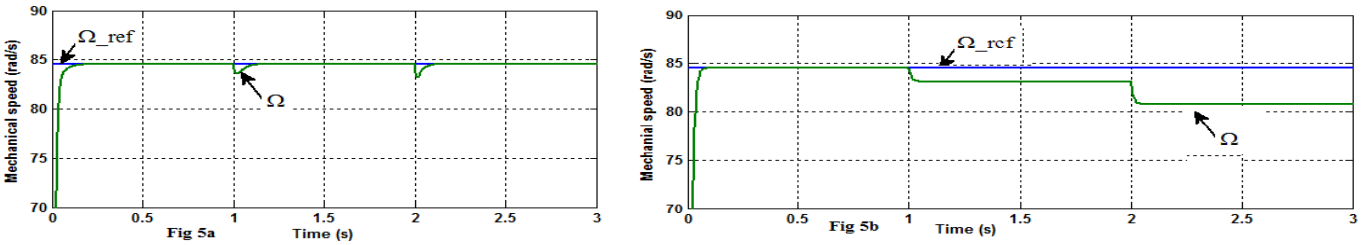

Fig.5: Speed regulation performance of conventional and adaptive controllers
($I_{d\text{-}Ref}$=10A,v_{wind}=8m/s)

6. Conclusion

This paper has demonstrated the effectiveness and robustness of a nonlinear adaptive backstepping controller for Variable-speed DFIG system. The mathematical development was examined in detail for current and speed controllers. The speed tracking performance under unknown mechanical parameters was investigated by numerical simulation which has shown satisfactory performances of the proposed controller.

Appendix: Characteristics and Parameters

Induction Generator	
Rated power	1.5MW
Rated stator voltage	332/575V
Nominal frequency	50Hz
Number of pole pairs	p =3
Rotor resistance	R_s=0.0014Ω
Stator resistance	R_r=0.001Ω
Stator inductance	L_s=0.0019H
Rotor inductance	L_r=0.0019H
Mutual inductance	L_m=0.0018H
Wind Turbine	
Rated power	1.5MW
Blade Radius	R=17.4m
Power coefficient	C_{pmax}= 0.48
Optimal relative wind speed	λ_{opt}=8.1
Mechanical speed multiplier	G=22.5
Generator and Turbine	
Moment of inertia	J=1.9Kg .m^2
Damping coefficient	f=1.52

References

[1] H. Li, Z. Chen, "Overview of different wind generator systems and their comparisons" IET Renewable Power Generation, 2008, 2(2):123-138.

[2] F. Blaabjerg, R. Teodorescu, M. Liserre, "Overview of Control and Grid Synchronization for Distributed Power Generation Systems", IEEE Transaction on Industrial Electronics, 2006, 53(5):1398-1409.

[3] J. -J. Slotine, Applied nonlinear control, Printice Hall, 1996.

[4] A. R. Benaskeur, Aspects de l'application du backstepping adaptatif à la commande décentralisée des systèmes non-linéaires. PhD thesis, Department of Electrical and Computer Engineering, Université Laval, Quebec City, Canada, 2000.

[5] I. Kanellakopoulos, P.V. Kokotovic, and A.S. Morse, "Systematic design of adaptive controller for feedback linearizable systems", IEEE Trans. Auto. Control. 1991. Vol. 36, (11), pp. 1241-1253.

[6] Siegfried Heier, "Grid Integration of Wind Energy Conversion Systems," John Wiley & Sons Ltd, 1998, ISBN 0-471-97143-X

[7] R. Pena, J.C.Clare, G. M. "Asher Doubly fed induction generator using back-to-back PWM converters and its application to variable-speed wind-energy generation" IEE Pvoc.-Electr. Power Appl, Vu1 143, No. 3, May 1996

[8] H. Tan, J. Chang, "Field orientation and adaptive backstepping for induction motor control"IEEE Proc. 1999.

[9] BOUSSERHANE , BOUCHETA , HAZZAB, MAZARI, RAHLI, FELLAH Adaptative backstepping Controller Design For Lineair Induction Motor Position Control U.P.B. Sci. Bull., Series C, Vol. 71, Iss. 3, 2009, ISSN 1454-234x.

[10] A. Tapia, G. Tapia, J. Ostolaza and J. saenz, Modeling and control of a wind turbine driven doubly fed induction generator, IEEE Trans. On Energy Conversion, vol. 18, no2, pp. 194-204, June 2003.

[11] P. Andreas, H. Lennart and T. Torbjorn, Evaluation of Current Control Methods for Wind Turbines Using Double-Fed Induction Machines, IEEE Trans. on Power Electronics, Vol. 20, n°1, pp 227-235, January 2005.